Journal of
Applied Crystallography
ISSN 0021-8898

Received 16 August 2006
Accepted 28 February 2007

Living anionic polymerization of methyl methacrylate controlled by metal-free phosphazene catalyst as observed by small-angle neutron scattering, gel-permeation chromatography and UV–visible spectroscopy

Nobuyoshi Miyamoto,[a,b]* Yoshihisa Inoue,[c] Satoshi Koizumi[a] and Takeji Hashimoto[a]

[a]Advanced Science Research Center (ASRC), Japan Atomic Energy Agency (JAEA), Shirakata-Shirane 2-4, Tokai-mura, Ibaraki 319-1195, Japan, [b]Department of Life, Environment and Materials Science, Fukuoka Institute of Technology, 3-30-1, Wajiro-Higashi, Higashi-ku, Fukuoka 811-0295, Japan, and [c]Catalysis Science Laboratory, Mitsui Chemicals Inc., Nagaura 580-32, Sodegaura, Chiba 299-0265, Japan. Correspondence e-mail: miyamoto@fit.ac.jp

Phosphazene (PZN) catalyst, PZN catalyst coexisting with a co-catalyst 1-hydroxycyclohexyl phenyl ketone (Irgacure 184; IRG) and polymethylmethacrylate (PMMA) (prepared by catalytic living anionic polymerization using the PZN catalyst and IRG) have been observed for the first time by small-angle neutron scattering (SANS) and UV–visible spectroscopy to elucidate the aggregation behavior of the PZN molecules themselves and the state of living chain ends in a living polymer solution. PZN catalyst in deuterated tetrahydrofuran (thf-d_8) showed SANS curves fitted by a form factor for a sphere whose radius R_s is larger (1.4–1.6 nm) than a single PZN molecule (0.65 nm), indicating formation of PZN aggregates in thf-d_8. In a nonpolar solvent, benzene-d_6, R_s was even larger (3.1 nm), indicating formation of larger aggregates. By adding IRG to PZN solution, an excess scattering appeared in the SANS profile and a strong band emerged in the UV–visible spectrum. This result indicates strong interaction of IRG with PZN not only on a molecular scale but also on a mesoscopic scale. The SANS profile from the living polymer solution in thf-d_8 was observed to be fitted by the sum of the profile for the aggregated PZN/IRG complex and that for Gaussian chains of PMMA. The molecular weight of the PMMA determined by SANS, 2100 g mol^{-1}, was in agreement with that estimated from gel-permeation chromatography, indicating that the anionic living chain ends and their counter ions (PZN) are dissociated in thf-d_8; thus, the chains are not associated into multiple-ion pairs.

1. Introduction

Living anionic polymerization is an established method for synthesizing polymers with a very narrow molecular weight distribution and specific structures such as starpolymers and block copolymers. Living anionic polymerization is usually conducted by using an initiator such as an alkyllithium compound. However, this method is industrially disadvantageous because one initiator molecule produces only one polymer chain, so a large amount of costly initiator is necessary. Further, metals in the initiator remain in the products, leading to unfavorable properties.

Nobori *et al.* recently found that polymerization of methyl methacrylate (MMA; Fig. 1c) proceeds in a *catalytic living anionic polymerization manner*, like so-called immortal polymerization (Aida *et al.*, 1988), in the presence of the metal-free phosphazenium salt of active hydrogen (PZN; Fig. 1a) and an alcoholic chain transfer agent (Nobori *et al.*, 1999). As shown in Fig. 2, a large number of propagating chains [species (a) to (d) in Fig. 2] are formed with a small

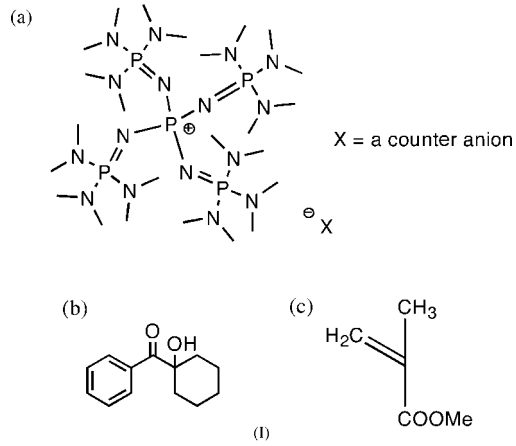

Figure 1
(a) PZN catalyst, (b) Irgacure 184 (IRG) and (c) methyl methacrylate (MMA).

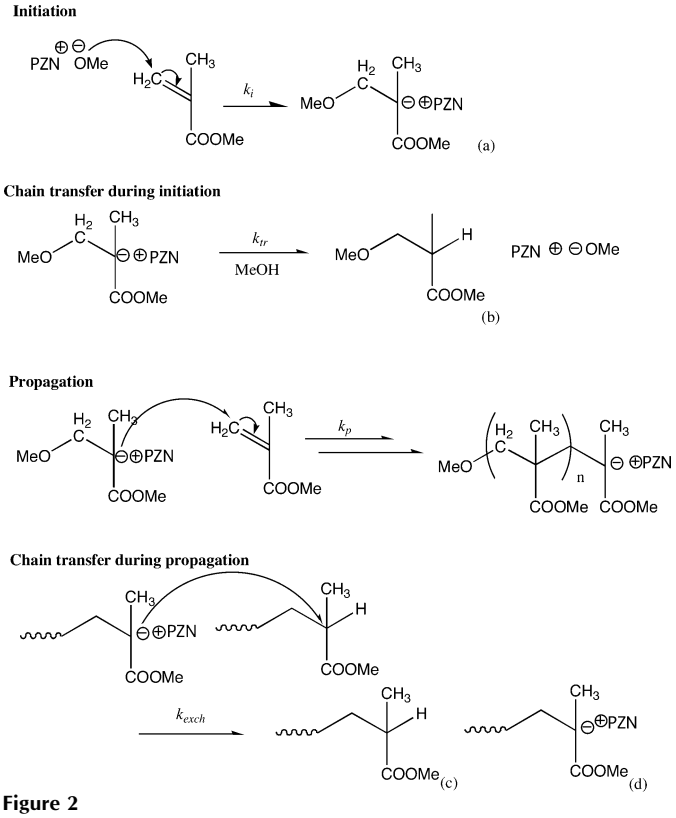

Figure 2
Reaction scheme for catalytic living anionic polymerization of polymethylmethacrylate in the presence of a phosphazenium compound and Irgacure. The reaction proceeds in a living manner under the condition $k_p << k_{tr}$ and $k_p << k_{exch}$.

number of the initiator (catalyst) molecules through fast transfer of the active sites during the initiation step and in the propagation step. During the propagation step, the anionic active living ends are quickly transferred among all the propagating polymer chains [species (c) and (d) in Fig. 2]. The product polymers have high molecular weight and narrow molecular weight distribution (Nobori *et al.*, 2004; Takaki *et al.*, 2003). However, details of the reaction mechanism such as interactions between PZN and the propagating living chain end have not been elucidated yet.

In living anionic polymerization, superstructures formed by catalyst (or initiator) molecules and/or living polymer chain ends have crucial effects on the control of the reactions. For *in-situ* observation of superstructures on the length scales of sub-nanometres to micrometres appearing during chemical reactions, small-angle neutron scattering (SANS) is a powerful tool because of the low energy and high transmittance of neutrons. Recently, the aggregation behaviors of the anionic living ends in nonpolar solvents were analyzed by SANS (Stellbrink *et al.*, 1998; Niu *et al.*, 2005; Miyamoto *et al.*, 2006).

In this study, we utilize *in-situ* SANS combined with UV–visible spectroscopy and gel-permeation chromatography (GPC) in order to explore the living anionic polymerization of MMA catalyzed by PZN and a co-catalyst of 1-hydroxycyclohexyl phenyl ketone (Irgacure 184, denoted as IRG; Fig. 1b). We focus on elucidating the aggregation of the PZN catalyst, the interactions between PZN and IRG, and the state of living chain ends of the polymers.

2. Experimental

SANS measurements were carried out on SANS-J-II (Koizumi *et al.*, 2006) at the JRR3 research reactor, JAEA, Tokai, Japan. UV–visible spectra were measured concurrently with SANS by using the newly invented setup shown in Fig. 3: incident light from two light sources is guided by optical fibers to the collimation lens fixed to a sample cell made of quartz. The light transmits through the upper part of the cell and is collimated by another lens fixed to the cell to be guided through an optical fiber to a charge-coupled device (CCD)-type UV–visible spectrometer (Stellar Net Inc., EPP2000C).

A 2 mm thick cell connected to a glass tube was used for SANS and UV–visible spectroscopic measurements. The cell and tube were purged with Ar to avoid contamination by water, which deactivates the catalyst. The living anionic polymerization reaction was initiated by adding MMA monomer to the solution of PZN, methanol (the chain transfer agent) and IRG. We used deuterated tetrahydrofuran (thf-d_8) as the solvent to obtain enough SANS contrast between the solvent and nondeuterated PZN and MMA. Deuterated benzene (benzene-d_6) was also used to examine the influence of polarity of the solvent on the aggregation of PZN. PZN was synthesized according to the method previously reported (Nobori *et al.*, 1999) and obtained as a mixture of methanol, PZN-OH and PZN-OCH_3. IRG was purified by recrystallization from hexane. MMA, thf-d_8 and benzene-d_6 were well dried with Na or CaH and distilled under vacuum. The molecular weight of the obtained polymer was determined by GPC with a Tosoh GPC-8020 equipped with a refractive index detector. We used the following scattering length densities σ for the analyses of the SANS data: $\sigma_{\text{thf-}d} = 6.4 \times 10^{10}$ cm^{-2}, $\sigma_{\text{benzene-}d} = 5.4 \times 10^{10}$ cm^{-2} and $\sigma_{\text{PZN}} = 5.7 \times 10^{9}$ cm^{-2}.

3. Results and discussion

3.1. Aggregation of PZN catalyst

SANS profiles of PZN/thf-d_8 solutions revealed that PZN forms aggregates in thf-d_8. Curves (a)–(e) in Fig. 4 show the SANS profiles of the PZN/thf-d_8 solutions as a function of PZN concentration [PZN]. Whereas thf-d_8 shows q-independent scattering [q is the modulus of the scattering vector defined as $q = (4\pi/\lambda)\sin(\theta/2)$ with scattering angle θ and the wavelength of neutron beam λ], q-dependent curves emerged with increasing [PZN]. The measured SANS curves were fitted with the model function for a spherical particle with radius R_s,

$$I(q) = A_s P_{\text{sphere}}(qR_s) + I_{\text{BG}}, \quad (1)$$

where

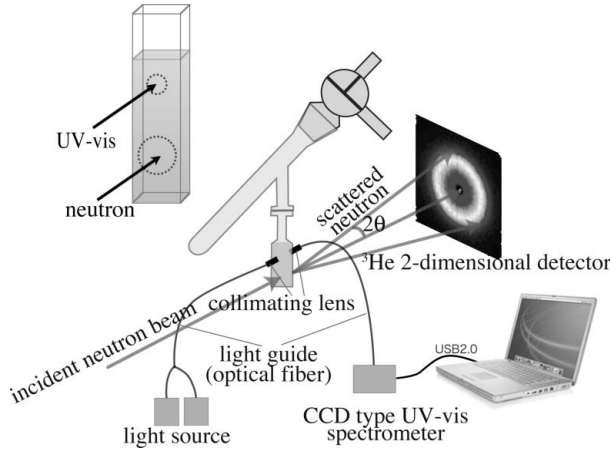

Figure 3
Setup for a simultaneous measurement of SANS and UV–visible spectra. The light sources are an Hg lamp (190–500 nm) and a tungsten–krypton lamp (350–1700 nm).

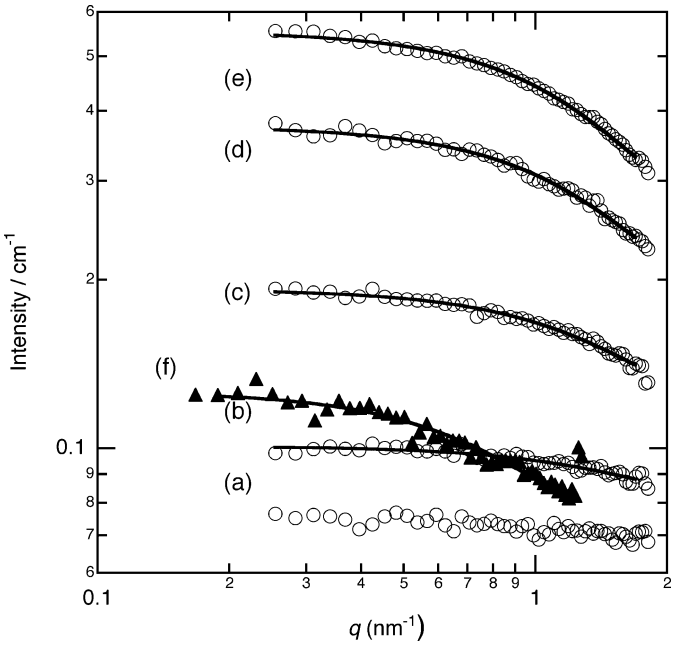

Figure 4
SANS profiles of (a) thf-d_8, (b)–(e) PZN/thf-d_8 solutions and (f) PZN/benzene-d_6 solution. [PZN] = (b) 0.5, (c) 2.0, (d) 5.0, (e) 8.0 and (f) 1.0 wt%. The solid lines are the best-fitted curves based on the theoretical scattering function for a dilute sphere dispersion [equation (1)].

$$P_{\rm sphere}(qR_{\rm s}) = (9/q^6R_{\rm s}^6)\left[\sin(qR_{\rm s}) - qR_{\rm s}\cos(qR_{\rm s})\right]^2,$$

$A_{\rm s}$ is a prefactor which depends on the contrast factor, the concentration of the particle and the volume of the sphere. $I_{\rm BG}$ is q-independent background scattering due mainly to incoherent scattering. By fitting with $A_{\rm s}$, $I_{\rm BG}$ and $R_{\rm s}$ as the floating parameters, we obtained $R_{\rm s}$ = 1.4–1.6 nm (Fig. 5a). We note that similar values of $R_{\rm s}$ were also obtained from Guinier analysis. $R_{\rm s}$ thus estimated is much larger than $R_{\rm s} \simeq 0.65$ nm evaluated by *Chem3D* software based on the molecular structure of PZN (Fig. 1a). This disagreement indicates that the PZN molecule is not molecularly dispersed but is present as aggregates in the solution. We suppose that van der Waals attractive interactions can promote aggregation of PZN molecules. Dipole–dipole attractive interactions may also cause aggregation when dissociation of the ion pair of the PZN cation and its counter anion into free ions is incomplete. Although electrostatic repulsion between positively charged PZN molecules prevent aggregation, this may not be the case for the present system because the charge density of PZN is very low.

Fig. 5(b) shows the $I_{\rm BG}$ values obtained by fitting as a function of [PZN]. From this plot, we estimated the experimental values of q-independent background scattering intensities for thf-d_8 and PZN as 0.071 and 2.6 cm^{-1}, respectively.

The aggregation was further promoted in the nonpolar solvent benzene-d_6; this supports the aggregation behavior of PZN in thf-d_8 discussed above. The profile (f) in Fig. 4 shows the result for the PZN/benzene-d_6 solution ([PZN] = 1.0 wt%). By fitting the profile in the same way as in the thf-d_8 system, we obtained $A_{\rm s}$ = 0.045 cm^{-1}, $R_{\rm s}$ = 3.1 nm and $I_{\rm BG}$ = 0.084 cm^{-1}. The large $R_{\rm s}$ indicates that the PZN aggregates in benzene-d_6 are larger than those in thf-d_8. We suppose that stronger attractive interactions between PZN molecules are present in benzene-d_6 than in thf-d_8 and the aggregation is promoted. Although $R_{\rm s}$ is larger in benzene-d_6, we find no large difference in $A_{\rm s}$ ($A_{\rm s}$ = 0.05 cm^{-1} from Fig. 5c for the PZN/thf-d_8 system with [PZN] = 1.0 wt%). We suppose that the number of PZN molecules in the aggregate is smaller in benzene-d_6 than in thf-d_8.

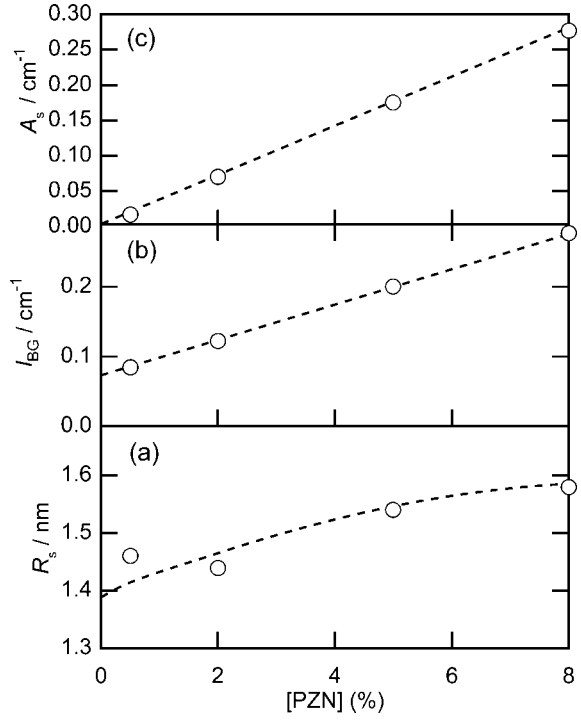

Figure 5
Parameters (a) $R_{\rm s}$, (b) $I_{\rm BG}$ and (c) $A_{\rm s}$ obtained by fitting the SANS curves for PZN/thf-d_8 solutions.

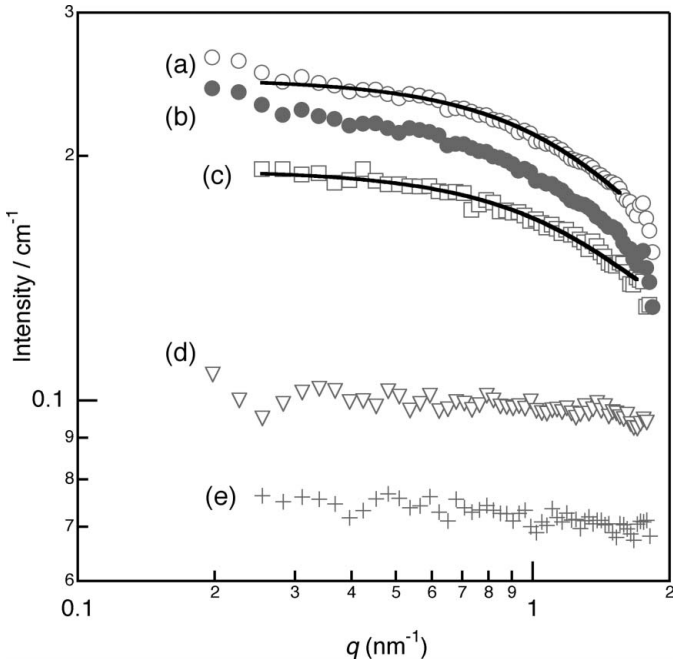

Figure 6
SANS profiles for (a) PZN/IRG/thf-d_8 ([PZN] = 2 wt% and [IRG] = 2 wt%), (c) PZN/thf-d_8 ([PZN] = 2 wt%) and (d) IRG/thf-d_8 ([IRG] = 2 wt%) solutions. Profile (b) was obtained by subtracting q-independent scattering of IRG from profile (a). The profile for thf-d_8, (e), is also shown for comparison. The solid lines are the best-fitted curves based on the theoretical scattering function for a dilute sphere dispersion [equation (1)].

3.2. The interaction between PZN and IRG

The addition of the co-catalyst IRG is crucial in controlling the living anionic polymerization reaction catalyzed by PZN and to obtain polymers with narrow molecular weight distribution. Here we explored the interaction of PZN and IRG by SANS and UV–visible spectra.

Firstly, the state of IRG alone was examined by SANS. In the SANS profile of an IRG/thf-d_8 solution [curve (d) in Fig. 6], only a q-independent scattering is observed. This indicates that IRG is molecularly dispersed in the solvent. The scattering intensity is larger by 0.011 cm^{-1} than that of thf-d_8 [curve (e) in Fig. 6]. The excess in the scattering intensity is ascribed to incoherent scattering from IRG and coherent scattering from concentration fluctuations of IRG and thf-d_8.

Next, IRG was added to a PZN/thf-d_8 solution and the SANS profile was measured [curve (a) in Fig. 6]. Even after subtracting q-independent scattering of IRG from the profile of the PZN/IRG/thf-d_8 solution [curve (b) in Fig. 6], we still observe an excess scattering compared to the PZN/solution [curve (c) in Fig. 6]. This result indicates that PZN and IRG are interacting to form complexes on the mesoscopic scale. The curves (a) and (c) in Fig. 6 were fitted by equation (1) with R_s and A_s as floating parameters and I_{BG} fixed to 0.14 and 0.12 cm^{-1}, respectively, based on the experimental values. The fitting results are shown as the solid lines in Fig. 6. A_s was 0.07 and 0.11 cm^{-1} for the curves before and after adding IRG, respectively, while the corresponding R_s values are 1.4 and 1.5 nm. Thus, only A_s increases upon the addition of IRG, whereas R_s is kept unchanged. We attribute this to the increase in the contrast factor of the PZN aggregate *versus* the solvent by incorporation of IRG into the PZN aggregate without modifying the overall structure.

The UV–visible spectrum was also changed by adding IRG to PZN/thf-d_8. IRG/thf-d_8 showed a maximum at around 330 nm [curve (c) in Fig. 7], which is due to an n–π^* transition of the C=O group in the IRG molecule, whereas the PZN/thf-d_8 solution shows no peak in the measured range [curve (d) in Fig. 7]. By adding PZN to IRG, the band at 330 nm was replaced by a stronger band at around 360 nm [curve (a) in Fig. 7], indicating the formation of a complex by the association of IRG with the active PZN catalyst.

By exposing the PZN/IRG/thf-d_8 solution to air, water is introduced and PZN is deactivated. Upon deactivation, the band at 360 nm in the UV–visible spectrum disappeared and only a weak band at 330 nm remained [curve (b) in Fig. 7]. In contrast, no change was found in the SANS profile upon deactivation. Thus, the microscopic structure of PZN/IRG was changed upon deactivation, whereas the mesoscopic scale superstructures of PZN/IRG were not affected by deactivation of the catalyst.

3.3. The state of the catalyst and polymer chains during the living anionic polymerization reaction

By adding monomer to PZN/IRG/thf-d_8 solution, the living anionic polymerization was initiated and the reaction completed in several minutes. GPC measurements showed that the polymer obtained had a number average molecular weight M_n of 2300 g mol^{-1}, which was in good agreement with the theoretically predicted value, $(M_{MMA}[MMA])/([MeOH] + [PZNOMe]) = 2500$ g mol^{-1}. The fairly narrow molecular weight distribution having $M_w/M_n = 1.23$ shows that the reaction is controlled in a living manner; the molecular weight distribution will be improved by optimization of the reaction conditions in future. In experiments on a separate batch, we confirmed that, while keeping a narrow molecular weight distribution, the molecular weight increases upon stepwise addition of the monomer. Thus, the reaction proceeded in a controlled living manner.

To elucidate the interaction between the living polymer ends and the catalyst molecules, we measured SANS profiles (Fig. 8). Since the reaction was very fast and completed before beginning the measurements, the data shown here are for the living polymer solution in a fully polymerized state (M_n = 2300 g mol^{-1}) with no MMA

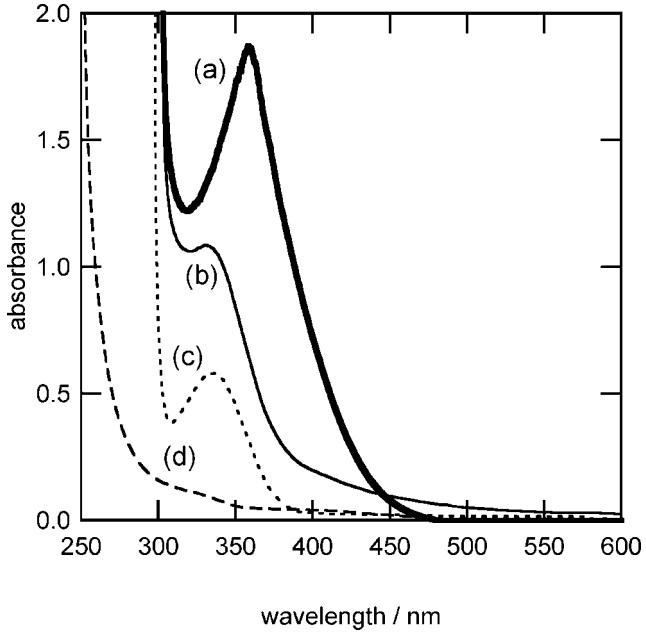

Figure 7
UV–visible spectra of PZN/IRG/thf-d_8 solution (a) before and (b) after deactivation of the catalyst, (c) IRG/thf-d_8 solution and (d) PZN/thf-d_8 solution. [PZN] = 1.6 wt% and [IRG] = 0.5 wt%.

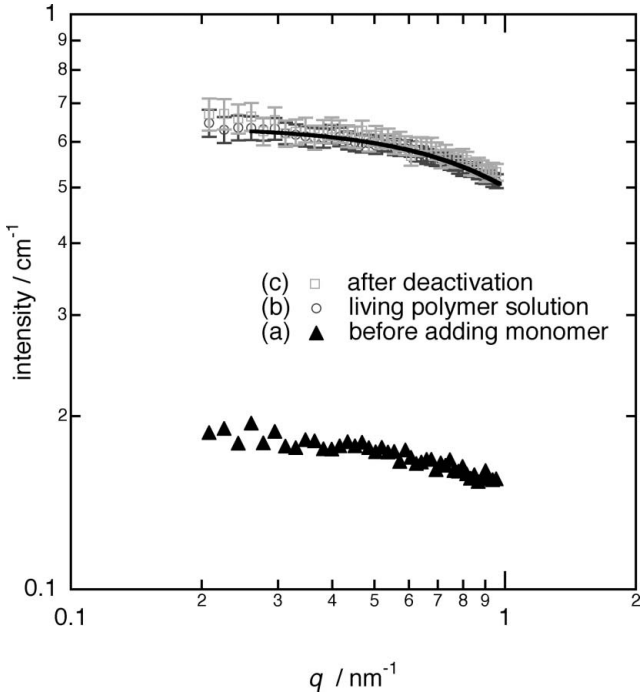

Figure 8
SANS profiles of the living polymer solution ([PZN] = 1.5 wt%, [IRG] = 0.5 wt%, [MMA] = 9.4 wt%) in thf-d_8 (b) before and (c) after deactivation. The SANS profile before adding the monomer (a) is also shown.

remaining as confirmed by GPC. Compared to the profile before adding the monomer [curve (a) in Fig. 8], the scattering intensity largely increased on completion of the reaction [curve (b) in Fig. 8], indicating the formation of polymer chains.

The scattering curve of the living polymer solution was fitted by the following function, which describes a mixture of spheres [equation (1)] and Gaussian chains with a radius of gyration R_g:

$$I(q) = A_s P_{sphere}(q, R_s) + A_g P_g(q, R_g) + I_{BG}, \quad (2)$$

where

$$P_g(qR_g) = (2/q^4 R_g^4)\left[q^2 R_g^2 - 1 + \exp(-q^2 R_g^2)\right]$$

and A_g is the prefactor concerning the concentration and molecular weight of the polymer and the contrast factor between the polymer and the solvent. Upon fitting the curve, I_{BG} was fixed to 0.12 and 0.26 cm^{-1} for the curves (a) and (b), respectively, based on experimentally determined values. By fitting curve (a) of Fig. 8 (before adding monomer) with equation (1), the parameters for the PZN aggregate were first determined as $R_s = 1.8$ and $A_s = 0.08$. Finally, by fitting the curve after adding monomer [curve (b) in Fig. 8] with equation (2), along with the data obtained on R_s and A_s, we obtained $A_g = 0.35$ cm^{-1} and $R_g = 1.1$ nm, which corresponds to the molecular weight $M_{SANS} = (R_g/K)^2 = 2100$ g mol^{-1} with $K = 0.024$ [obtained experimentally by measuring the thf-d_8 solution of a polymethylmethacrylate (PMMA) with known molecular weight]. M_{SANS} is in agreement with the values evaluated from GPC (2300 g mol^{-1}) and theoretical calculations (2500 g mol^{-1}).

Termination of the reaction caused no remarkable change in the SANS profile, as shown in curve (c) in Fig. 8. The living polymers were terminated by the reaction with water by exposing the solution to air. Upon termination, a large change in the UV–visible spectrum was observed. In the living polymer solution [curve (a) in Fig. 9], a band at 360 nm, ascribed to IRG coexisting with active PZN catalyst, was observed. After termination [curve (b) in Fig. 9], this band disappeared and only a weak band at 330 nm due to IRG/thf-d_8 remained. In contrast to the large change in the UV–visible spectra, we find no difference between the SANS profiles before [curve (b) in Fig. 8] and after [curve (c) in Fig. 8] termination over the q range covered in this experiment.

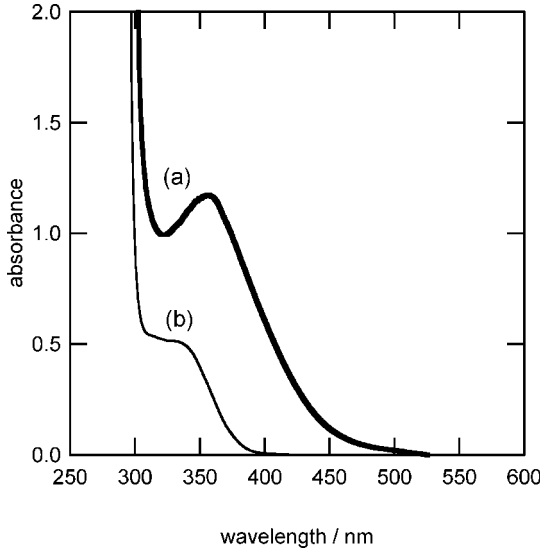

Figure 9
UV–visible spectra of the living polymer solution (a) before and (b) after deactivation.

The above results indicate that the living polymers prepared by PZN and IRG in thf-d_8 are present as nonaggregated chains. This is in contrast to the reports (Stellbrink *et al.*, 1998; Niu *et al.*, 2005; Miyamoto *et al.*, 2006) on conventional living anionic polymerization in nonpolar solvents with alkyllithium compounds as an initiator: in this case, the anionic living ends of the polymers and the lithium cations form aggregates, which are characterized by SANS as *n*-armed star polymers, *via* electrostatic attraction. Upon termination reaction, the charges in the living ends are lost and the aggregates formed *via* electrostatic attraction also disappear. In the present case, however, the aggregation of anionic living ends was not observed at all, as evidenced by no changes in the SANS profiles before and after deactivation (although the q range covered may not be sufficiently wide). The absence of the aggregates of living chain ends should be one of the key factors for a fast reaction in this living anionic polymerization system.

4. Conclusions

PZN catalyst in thf-d_8 and benzene-d_6, a mixture of PZN and IRG in thf-d_8, and living anionic polymers of PMMA coexisting with PZN and IRG in thf-d_8 were explored by SANS and UV–visible spectroscopy. In the PZN/thf-d_8 solution, SANS results indicated that PZN is present as aggregates. Upon addition of IRG to PZN solution, both the UV–visible spectra and the SANS profiles changed greatly, indicating these two species form a certain complex both on the molecular scale and the mesoscopic scale. In the living polymer solution, the SANS profile was found to be fitted by the sum of the profiles for the aggregated PZN/IRG complex and single Gaussian chains of PMMA. The absence of the aggregate of the living chain ends and counter ions, the aggregate which is present in the living anionic polymerization by alkyllithium initiators in nonpolar solvents, should be a key factor for fast reaction in this living anionic polymerization. We would like to note that from our experience in this work the concurrent measurement of *in-situ* SANS and UV–visible spectroscopy for a sample in a single cell is crucial for the observation of variety of novel chemical reactions.

This work was partly supported by a Grant-in-Aid (No. 17750114) for Young Scientists from the Ministry of Education, Culture, Sports, Science and Technology, Japan.

References

Aida, T., Maekawa, Y., Asano, S. & Inoue, S. (1988). *Macromolecules*, **21**, 1195–1202.
Koizumi, S., Iwase, H., Suzuki, J., Oku, T., Motokawa, R., Sasao, H., Tanaka, H., Yamaguchi, D., Shimizu, H. M. & Hashimoto, T. (2006). *Physica B*, **385–386**, 1000–1006.
Miyamoto, N., Yamauchi, K., Hasegawa, H., Hashimoto, T. & Koizumi, S. (2006). *Physica B*, **385–386**, 752–755.
Niu, A. Z., Stellbrink, J., Allgaier, J., Willner, L., Radulescu, A., Richter, D., Koenig, B. W., May, R. P. & Fetters, L. J. (2005). *J. Chem. Phys.* **122**, 134906-1–134906-16.
Nobori, T., Funaki, K., Shibahara, A., Suzuki, M., Mizutani, K., Jouyama, H., Hara, I., Hayashi, T., Kiyono, S., Fujiyoshi, S., Sakayama, H., Mizoguchi, M., Matsumoto, T. & Hirose, Y. (2004). Mitsui Chemicals, Inc. US Patent 6 762 259.
Nobori, T., Kouno, M., Suzuki, T., Mizutani, K., Kiyono, S., Sonobe, Y. & Takaki, U. (1999). Mitsui Chemicals, Inc. US Patent 5 990 352.
Stellbrink, J., Willner, L., Jucknischke, O., Richter, D., Lindner, P., Fetters, L. J. & Huang, J. S. (1998). *Macromolecules*, **31**, 4189–4197.
Takaki, U., Hara, I., Mizutani, K., Kiyono, S., Nobori, T., Funaki, K., Hayashi, T. & Shibahara, A. (2003). Mitsui Chemicals, Inc. US Patent 6 528 599.